

NASA Contractor Report 191187
AIAA-93-2391

1N-20
186028
28 P

Low Power Pulsed MPD Thruster System Analysis and Applications

Roger M. Myers
Sverdrup Technology, Inc.
Lewis Research Center Group
Brook Park, Ohio

Matthew Domonkos
University of New Mexico
Albuquerque, New Mexico

and

James H. Gilland
Sverdrup Technology, Inc.
Lewis Research Center Group
Brook Park, Ohio

Prepared for the
1993 Joint Propulsion Conference
cosponsored by the AIAA, SAE, ASME, and ASEE
Monterey, California, June 28-July 1, 1993



(NASA-CR-191187) LOW POWER PULSED
MPD THRUSTER SYSTEM ANALYSIS AND
APPLICATIONS (Sverdrup Technology)
28 p

N94-13415

Unclass

G3/20 0186028

Low Power Pulsed MPD Thruster System Analysis and Applications

Roger M. Myers¹
Sverdrup Technology, Inc.
NASA Lewis Research Center
Cleveland, OH 44135

Matthew Domonkos²
University of New Mexico
Albuquerque, NM

and

James H. Gilland³
Sverdrup Technology, Inc.
NASA Lewis Research Center
Cleveland, OH 44135

Abstract

Pulsed MPD thruster systems were analyzed for application to solar-electric orbit transfer vehicles at power levels ranging from 10 to 40 kW. Potential system level benefits of pulsed propulsion technology include ease of power scaling without thruster performance changes, improved transportability from low power flight experiments to operational systems, and reduced ground qualification costs. Required pulsed propulsion system components include a pulsed applied-field MPD thruster, a pulse-forming network, a charge control unit, a cathode heater supply, and high speed valves. Mass estimates were obtained for each propulsion subsystem and spacecraft component using off-the-shelf technology whenever possible. Results indicate that for payloads of 1000 and 2000 kg pulsed MPD thrusters can reduce launch mass by between 1000 and 2500 kg over those achievable with hydrogen arcjets, which can be used to reduce launch vehicle class and the associated launch cost. While the achievable mass savings depends on the trip time allowed for the mission, cases are shown in which the launch vehicle required for a mission is decreased from an Atlas IIAS to an Atlas I or Delta 7920.

Nomenclature

C	capacitance of pulse-forming network, F
C _s	capacitance per stage of pulse-forming network, F
E _p	energy per pulse, J
g _o	acceleration of gravity, 9.8 m/s ²
I _{sp}	specific impulse, s
I _t	mission total impulse, N-s
L _s	inductance per stage of pulse-forming network
\dot{m}	propellant mass flow rate, kg/s, defined by Eqn. (6)
M _c	mass of capacitors in PFN, kg

¹ Propulsion Engineer, member AIAA

² Undergraduate student, member AIAA

³ Research Engineer, member AIAA

This paper is a work of the U.S. Government and is not subject to copyright protection in the United States.

M_f	final spacecraft mass, kg
M_{pay}	payload mass, kg
$M_{p.c.}$	propellant management system mass, kg
$M_{p.s.}$	propulsion system mass, kg
M_{pow}	power system mass, kg
M_{str}	structural mass, kg
N_p	total number of pulses required per thruster
N_s	number of stages in pulse-forming network
N_t	number of thrusters
P_p	peak power during pulse, W
P_t	thruster power, W
T_f	tankage fraction
V_p	thruster voltage during pulse, V
ΔV	mission velocity increment, m/s
Z_o	thruster discharge impedance, ohms
α_c	capacitor specific mass, kg/F
η_t	thruster efficiency
τ_p	pulse duration, s

Introduction

Magnetoplasmadynamic (MPD) thrusters have demonstrated performance and power handling capabilities which make them attractive for use on orbit transfer and planetary missions.¹⁻³ Testing has been done at power ranges from 10 kW to 600 kW on steady-state thrusters, and from 200 kW to 10 MW with pulsed thrusters with single pulse durations up to 10 ms. The simple and robust MPD thruster design permits operation at power densities exceeding those of other electric propulsion technologies. While most MPD thruster testing has been directed at applications requiring hundreds of kilowatts of power for propulsion, recent efforts have focussed on the potential for near-term application of MPD thruster technology at power levels below 40 kW, where previous studies have indicated that steady-state thrusters have poor performance characteristics for all propellants except lithium.^{1,2,4} Use of lithium may be precluded because of potential spacecraft contamination from the condensable propellant. These performance and integration limitations have led to the consideration of pulsed propulsion systems, in which the thrusters operate at constant peak power with a duty cycle dictated by the available spacecraft power.

Two experimental pulsed MPD thruster systems have been flown in space. The first of these,⁵ flown on the MS-T4 spacecraft in 1981, consisted of two applied-field MPD thrusters operating on ammonia propellant. The results indicated that ground performance measurements were correct, and that the 1.5 ms duration, 100 kW peak power discharges did not interfere with other spacecraft functions. The MS-T4 propulsion system power was 30 W, and the thrusters discharged about once every 32 seconds for a total of 400 discharges. The second flight demonstration, on the first Space Experiments with Particle Accelerators (SEPAC) Space Shuttle flight in 1985,⁶⁻⁸ utilized a much higher peak power discharge of 2 MW, and showed that very high power pulsed systems could be successfully integrated and flown on manned spacecraft. Neither of these flights utilized thrusters or systems with the performance and lifetime required for operational systems, but they were an important step in demonstrating the feasibility of integrating pulsed MPD thruster technology. Additionally, pulsed thrusters with up to 3 MW peak power and discharge durations of ~10 μ sec are being flown on the Navy NOVA spacecraft, and have demonstrated over 10 years of on-orbit lifetime.^{9,10} A large amount of work has been done to integrate pulsed electromagnetic propulsion on spacecraft, and no insurmountable issues have been discovered.⁹ The flight of the Japanese Electric Propulsion Experiment (EPEX) on the Space Flyer Unit, scheduled for launch in 1994, will demonstrate a pulsed

MPD thruster system on a 1 kW spacecraft. The thruster will use hydrazine propellant, and the peak pulse power is over 2 MW. The principal issue with this system appears to be the short pulse duration of 150 μ s, which reduces the fraction of injected propellant actually accelerated to below 50% and dramatically reduces the thruster performance.⁹ The EPEX propulsion system has passed both EMI and vibration qualification testing.¹¹

There are several potential advantages of pulsed MPD thruster systems, including power scaling without changes in thruster performance or size and reduced testing costs. Power scaling is accomplished via changes in pulse frequency, with no modification to the thruster or its operating conditions during a pulse. This means that thruster efficiency and specific impulse are unchanged as the power level changes, and that power restrictions resulting from either solar array degradation or increased distance from the sun will not impact thruster performance. This capability improves the transportability of data obtained on low-power flight tests to full-scale operational systems. The additional complexity of having an energy storage unit and high-speed valves may be offset by the ability of one or two thrusters to process all the power available for propulsion, reducing the need for a large number of thrusters. Finally, pulsed MPD thrusters will likely have reduced testing costs, since accurate performance measurements and integration tests can be made on a single or multiple pulse basis with pressures near the ultimate facility pressure, with long-term lifetime and thermal characterizations made at the higher facility pressures associated with continuous operation. MPD thrusters have been shown to be insensitive to facility pressure for values below 0.07 Pa, a value which is readily achievable in available large space simulation facilities for the time average propellant flow rates expected at power levels below 100 kW.¹

Potential near term applications of pulsed MPD thruster systems include primary propulsion for solar electric orbit transfer vehicles (SEOTVs) and planetary spacecraft which have an electric power capability of 10 to 40 kW. The goal of this study is to establish the power level and mass regimes for which pulsed MPD thrusters are competitive with hydrogen arcjets and to identify key technology requirements. Hydrogen arcjets were selected for comparison because of the similarity of the thruster propellants. A comparison with ion thrusters was beyond the scope of this work. Previous studies have been performed which examined the application of pulsed thrusters to 100 kW class nuclear electric propulsion systems. These efforts generally found that, given the technology available in the early 1980's, the mass of the energy storage system was such that pulsed MPD thrusters were ineffective at power levels much below 100 kW.^{12,13} In addition, cathode erosion in pulsed thrusters was found to be too high to achieve the long thruster lifetimes required.¹⁴ Since that time, however, considerable effort has gone toward the development of improved capacitors for pulsed power applications, and a new examination of the cathode lifetime has resulted in a potential solution to the lifetime limitations.

This paper presents an analysis of pulsed MPD thruster systems including recent technology developments. The components of a pulsed MPD thruster system are described first, including the thruster, power management, thermal control, and propellant storage and distribution systems. Mass estimates are developed for each component valid for power levels between 10 kW and 40 kW. Spacecraft integration issues are then discussed in the context of previous flight experience. The results of the mass analysis are used in a simple mission model to establish benefits for pulsed MPD thrusters by comparing them with hydrogen arcjets. The sensitivity of the initial spacecraft wet-mass to thruster and power processor performance are examined. Finally, a summary of the major conclusions of this study is provided.

System Components

Pulsed propulsion technologies will only be used if they offer sufficient mission and development cost benefits to offset the added complexity of the high-speed valves and energy storage system. While continuous propellant feed systems have been proposed to eliminate the high speed valve,¹⁵ this technique is not considered in this study due to the high repetition rates ($\sim 10^4$ Hz) required to maintain high propellant utilization efficiency. The propellant utilization efficiency in continuous feed systems also couples the thruster length, performance, pulse power, and spacecraft power, which compromises the ability of pulsed systems to accommodate spacecraft power changes

without simultaneous changes in thruster performance. A simple schematic of the pulsed propulsion system considered in this work is given in Fig. 1, where the charge control unit, CCU, serves as the interface between the spacecraft bus and the pulse forming network, and the cathode heater supply maintains a sufficiently high cathode temperature to ensure thermionic emission. For all pulsed systems, the mass of the energy storage unit is determined by its specific energy and the energy per pulse, where the latter is determined by the total mission energy change and the total number of pulses. Thus, the relative merits of pulsed and steady-state systems will be determined by the mission requirements, the performance of the different thrusters, and the system masses. While it is premature to specify a thruster or system design, this section describes the component design criteria and presents a point design which is used as a basis for comparisons with hydrogen arcjets.

Thruster

The thruster includes the electrodes, applied-field magnet, insulators, propellant injection system, and any heat rejection hardware required by these elements. The highest pulsed MPD thruster performance measured to date has been obtained at Princeton University using a self-field thruster¹⁶ and at Osaka University using an applied-field thruster.¹⁷ Both thrusters used hydrogen propellant, and their efficiency exceeded approximately 50% at 7000 s I_{sp} . While this I_{sp} is too high for optimal LEO-GEO transfer times, there are several options currently being explored to reduce the I_{sp} while maintaining the efficiency. These include the use of deuterium or lithium propellants, geometry changes, and optimizing the shape and strength of the applied magnetic fields. Deuterium has been used in tests at the Los Alamos National Laboratory, and simple performance estimates indicate efficiencies near 50% at 5000 seconds I_{sp} .¹⁸ Lithium, while not yet tested in pulsed thrusters, has yielded performance levels over 60% efficiency at 5000 s I_{sp} at a power level of 20 kW.⁹ Work in Japan and the United States has shown that thruster performance can be significantly improved via changes in thruster geometry, including flaring the anode, shortening the cathode, and modifying the propellant injection.^{1,2} Applied magnetic fields have been extensively studied in the United States, Japan, and the former Soviet Union, and have been found to increase thruster performance for both steady-state thrusters at power levels up to 200 kW and pulsed thrusters at peak power levels of several megawatts.⁹ However, the complex physics governing operation of applied-field MPD thrusters has to date precluded thruster optimization. Only recently have the experimental data base and numerical codes approached the level required to permit reasoned approaches to applied-field MPD thruster design.^{1,9,19}

For this study the thruster geometry was based on the Princeton thruster^{14,16} with modifications made both to accommodate an applied magnetic field and to achieve the required lifetime. The Princeton benchmark thruster has an anode radius of 5 cm, a cathode radius of 0.9 cm, and a chamber length of 10 cm. The electrode geometry was modified to accommodate the 2500 - 6000 hour lifetime required for the LEO - GEO transfer missions. The principal life-limiter in these thrusters is the cathode, principally as a result of operation at current densities beyond the material capability or at too low a surface temperature.¹⁴ Cathodes operated properly have demonstrated lifetimes over 12,000 hrs at current densities of 20 - 30 A/cm² under vacuum conditions.^{20,21} These results were obtained using porous tungsten impregnated with a 4:1:1 molar mixture of BaO, CaO, and Al₂O₃ operated at 1050 °C. A peak discharge current of 7.5 kA was selected for this study, yielding a required emitting surface area of 375 cm² for an emission current density of 20 A/cm². Assuming that the cathode surface can be textured or grooved so as to increase the emitting surface area by a factor of two and that the uniform surface temperature results in uniform arc attachment, the cathode radius and length should be 1.6 cm and 17 cm, respectively. The cathode wall thickness was arbitrarily set to 0.64 cm. The anode geometry was chosen to be a straight cylinder 6.5 cm in radius and 17 cm long, though use of a flared anode such as those used in several Japanese studies would not strongly affect the results. Although it is likely that a lighter weight, higher conductivity material could be used, molybdenum was selected as the anode material because it would yield a conservative weight estimate. The anode wall thickness was set to 0.3 cm. These thruster components are illustrated in Fig. 2.

The surface temperature of barium impregnated tungsten cathodes must be maintained at a uniform temperature of about 1050 °C to ensure adequate thermionic emission.²⁰ This will be accomplished by imbedding a heater inside the cathode. Several heater designs have demonstrated operation at over 1100 °C for several thousand hours, including

heaters currently used on flight qualified resistojets and heaters that have flown on ion thrusters. Resistojet heaters designed to survive exposure to oxidizing propellants have been tested at temperatures over 1000 °C for 10,000 hrs.²² The heater power requirement for this study was estimated from the sum of the radiated and conducted power away from the cathode. The radiated power was calculated assuming that the anode temperature was equal to the cathode temperature, a condition which will be shown to be reasonable, and that the backplate surface temperature was 300 °C cooler than the cathode. The appropriate view factors were calculated, and it was found that the cathode radiated between 240 and 470 W, depending on the impact of the surface texturing on the effective radiating area. Heat conduction was estimated to be between 150 and 200 W depending on the required wall thickness of the cathode base, yielding a total heater power requirement of between 390 and 670 W. The performance loss resulting from ohmic dissipation in the thin walls of the cathode base was found to be negligible, though the structural implications were not examined.

The anode and radiator size were determined from the requirement that all power deposited into the anode be radiated at the anode temperature. For peak power levels between 1.5 - 2.5 MW the fraction of input power deposited into the anode was between 25 and 35 percent with argon propellant.²³ Propellant and applied-field effects studies for both pulsed and steady-state thrusters^{24,25} have shown that the anode power fraction is lower with hydrogen propellant than with argon and that it decreases with increasing applied-field strength and input power. The lowest reported value is 21% at a pulsed input power of 1.1 MW.²⁵ For this study the anode power fraction was assumed to be 30 percent. Using a wall thickness of 0.25 cm and an emissivity of 0.8 the anode was found to be capable of radiating all of the absorbed power for average power levels of 40 kW or below without the need for an additional radiator. At the maximum average power of 40 kW the anode surface temperature was 1045 °C, which confirms that the anode and cathode temperatures can be near equal. The anode temperature could be reduced by extending a radiator fin off the front of the anode if necessary. Anode life has been found to be limited by sputtering for high molecular weight propellants such as argon and by localized melting when the thruster is operated at too high a current level.²⁶ Minimal sputtering should occur when using hydrogen, deuterium, or lithium propellants with refractory metal anodes.²⁶ Localized melting can be avoided by operating at lower peak current levels and by manufacturing the anode out of a high thermal conductivity material. The latter solution was found to be very effective in teflon propellant pulsed plasma thrusters at peak power levels over 3 MW, in which the lowest anode erosion rate was measured with a copper anode.²⁷

The substantial benefits observed with applied magnetic fields led to their inclusion in this study. Pulsed applied-field thrusters with the solenoid connected in series with the thruster discharge have been tested in Japan,^{2,17,25,28,29} and the principal thruster modification required was to ensure that the applied magnetic field can diffuse through the anode in a time short compared to the discharge time. This has been successfully accomplished for one millisecond discharges by cutting the anode axially and using thin walled anodes,^{17,25,28,29} and thus should not be a problem for the longer discharge times considered in this work. For this study the design of the applied-field coil was dictated by the desired field strength and the thruster discharge current. Previous studies using applied-field strengths of up to 0.2 T with steady-state thrusters show that the performance improves monotonically with field strength. Based on these results, a value of 0.2 T was selected for this study, and the coil radius was chosen such that a gap of 4 cm was left between the thruster anode and the coil. This gap can be used for radiation shields which will be needed to limit radiative heat transfer from the anode to the magnet. A preliminary estimate of the number of turns required in the applied-field coil was obtained using a model which an infinitely long solenoid. The result was then used in a finite length solenoid code developed by LaPointe³⁰ to establish accurate coil requirements. The coil was designed to be self-cooling by using flat copper stock to increase its surface area. The coil temperature was found by equating the average ohmic power deposition into the coil with the radiative heat loss. For the selected current level of 7.5 kA and a spacecraft power level of 40 kW, it was found that 5 turns of 2 cm wide, 0.5 cm thick copper would provide the required magnetic field and would self-cool at a temperature below 100 °C if coated to achieve an emissivity of 0.8. It is clear from this result that pulsed applied-field MPD thrusters will not require the development of new materials for the external solenoid.

A major difficulty with pulsed propulsion systems has been the achievement of high propellant utilization

efficiency.³¹ Propellant utilization efficiency is defined as the fraction of the total propellant injected per pulse which participates in the discharge. Achievement of high propellant efficiency has required the development of fast, extremely reliable valves and careful design of the propellant feed system to minimize the "dead volume" between the valve and the thruster. The controlling variables for propellant efficiency are the required pulse shape, trapped volume size, the pressure in the trapped volume, the pulse duration, and the propellant type. Only square propellant pulses were considered in this work. In this case, the trapped volume size and pressure should be minimized, the pulse duration maximized, and the propellant should be a low molecular weight gas. These rules lead to a reduction of the propellant mass which is not accelerated. The lower limit on the trapped volume pressure is determined by the requirement that the injection orifices be choked, and it can be varied by changing the mass flow rate and the total injection orifice area. Jones³¹ showed that a square propellant pulse is best achieved using a large valve orifice, a small total thruster orifice area, and a small trapped volume. The ratio of the valve orifice area to the thruster orifice area should be less than 0.5. In addition, increasing the thruster injection plenum temperature improves the gas efficiency by reducing the density of the gas in the trapped volume.

For this study the propellant injection geometry was designed to be similar to that used in the Japanese thrusters^{17,25,28,29} in which all propellant is injected around the cathode base, though scaled to accommodate the larger cathode diameter needed to ensure adequate lifetime. The result is shown in Fig. 2, where the trapped volume consists of the tube joining the high-speed valve to the annulus around the cathode base. The tube and annulus volume is approximately 6.2 cm³. The propellant efficiency was calculated as a function of discharge duration assuming that the current pulse ended at the same time as the high speed valve closed, which conservatively assumes that all the gas in the trapped volume is not accelerated. The result is shown in Fig. 3, from which it is seen that the propellant efficiency exceeds 98% for pulse durations over 2.5 ms for both hydrogen and deuterium propellants. For this work pulse durations between 1.5 and 2.5 ms were used for the system evaluation. Note that several groups in Japan have successfully improved the propellant efficiency by adjusting the timing of the current pulse such that it extends slightly beyond the valve closing, thus accelerating some of the gas in the trapped volume.^{17,25,28,29}

Considerable effort has gone into the development of high speed, high reliability valves over the past several years. The Japanese have developed a "Fast Acting Valve", FAV, which has operated reliably for over 3×10^6 pulses when used on an MPD thruster with a propellant mixture simulating hydrazine decomposition products.³² The FAV has opening and closing times of approximately 150 μ s and has resulted in pulsed MPD thrusters with apparently high propellant utilization efficiency with pulse durations of 1 ms. From another field, automobile fuel injector valves are built to cycle 6×10^8 times with a gas pulse duration of 2.5 ms and must remain within 6% of their start conditions for acceptance.³³ The latter is 2 to 3 times the number of cycles than will be required for a LEO - GEO transfer mission. Peak operating temperature for both of these valve is $\sim 100^\circ\text{C}$, so heat transfer to the valve results in a thermal control requirement. Both valves utilize less than 10 J per cycle. The Japanese FAV weighs 0.3 kg, and an automotive fuel injector valve weighs 0.1 kg.

The thruster and applied-field masses were estimated by summing the component masses and adding a 20% contingency. The component masses are given in Table 1, and the final result, for a thruster sized for a 40 kW spacecraft, is 11.3 kg, yielding a thruster specific mass of 0.3 kg/kW. The same thruster could be used without modification or performance degradation at lower power levels by simply modifying the pulse frequency. This capability permits very simple accommodation of decreasing spacecraft power during a mission resulting from array degradation. Of course, if the initial spacecraft power were decreased, then the anode, applied-field coil, and insulator masses could be reduced by using lighter materials and thinner walls.

Thruster Mounting Structure and Gimbals

Gimbals will likely be required on SEOTV's to minimize unwanted disturbance torques resulting from thrust vector misalignment.³⁴ Alternative reaction control systems are likely too heavy when sufficient propellant is included.³⁴ The thruster mounting structure mass is estimated as 30% of the thruster mass, and gimbal mass is modeled as 30% of the thruster mass plus the mounting structure mass.^{35,36,37} These relations yield a mounting structure and gimbal specific masses of 0.09 kg/kW and 0.12 kg/kW, respectively.

Power Management and Distribution

The power management and distribution system consists of the solar array, spacecraft bus, charge control unit, pulse forming network, cathode heater supply, and high speed valve supply. No igniter supply is needed for the proposed MPD thruster because the hot cathode is a ready supply of electrons. Low voltage ignition with heated cathodes has been well established.³⁸

Solar Array. - One near-term option for the solar array is the Advanced Photovoltaic Solar Array (APSA). Estimates of APSA specific mass show that unless strongly shielded it would start a LEO-GEO transfer mission at 8.3 kg/kW and end near 20 kg/kW,³⁹ so that an array with a beginning of life (BOL) power of 40 kW would have an end-of-life (EOL) power of 16.6 kW. Adding 0.03 cm of shielding reduces the fractional change in specific mass, but the array performance still degrades from 18 to 28 kg/kW over the course a 200 day transfer. The large degradation in array power which can be expected during the course of an orbit transfer mission reemphasizes the requirement for the propulsion system to accommodate power level changes without performance penalties. While there are alternative technologies which may improve the array specific mass to between 6.5 kg/kW (BOL) and 7.8 kg/kW (EOL),⁴⁰ this study assumed a constant value of 12 kg/kW for all propulsion system options. Time dependent array degradation was not included. In addition to the solar panels, a mechanism for panel deployment and orientation control must be provided. The mass of this system was estimated at 5.6 kg/kW, based on the results of a General Dynamics SEOTV study, which resulted in an overall solar power supply specific mass of 17.6 kg/kW.⁴¹

Charge Control Unit. - The charge control unit, or CCU, is very similar to an arcjet power processor unit (PPU) which operates at constant power. Current plans call for the Electric Propulsion Insertion Transfer Experiment (ELITE) spacecraft to incorporate a peak power tracker, which will yield a flight-packaged PPU specific mass of 3 kg/kW at 10 kW with 94% efficiency.⁴² In this study the CCU specific mass was set equal to that of an arcjet PPU and was assumed to be constant for power levels between 10 and 40 kW.

Cathode Heater Supply. - The cathode heater supply, CHS, is required to heat the cathode to 1050 °C so as to ensure adequate thermionic emission. The heater power requirement was determined above to be between 390 and 670 W. This power level will only be required during the start-up phase because discharge losses will supply a large fraction of the cathode heat once the thruster is operational. There are several efforts underway around the world to develop flight-qualified hollow cathodes which require heaters and the associated supplies.⁴³⁻⁴⁵ For this study, a high voltage heater was assumed and the CHS mass was set to 3 kg, which is equal to that of a flight-qualified 1 kW arcjet PPU which operates at 93 % efficiency.

Pulse Forming Network. - The largest additional component of a pulsed propulsion system is the energy storage unit or pulse-forming network (PFN). The PFN consists of a ladder network of capacitors and inductors tailored to provide the required current pulse shape and duration. To first-order, the PFN mass for a single string propulsion system is proportional to the energy per pulse, which is determined from the mission total impulse, the number of pulses per thruster, the number of thrusters required to perform the mission, and the thruster performance:

$$E_p = \frac{I_t I_{sp} g_0}{2 N_p N_t \eta_t} \quad (1)$$

which assumes a single string PFN/thruster system. Combining this result with the relationship for capacitor energy storage and introducing the capacitor specific mass, α_c , we obtain the approximate PFN capacitor mass:

$$M_c = \frac{I_t I_p g_o \alpha_c}{N_p N_t \eta_t V_p^2} \quad (2)$$

This equation illustrates the benefits of high voltage energy storage, providing that the capacitor specific mass is not too large and that the PFN can be matched to the thruster. Note that Equation (2) is not explicitly dependent on the pulse duration, which only enters in establishing the peak thruster power:

$$P_p = \frac{E_p}{\tau_p} \quad (3)$$

For a constant discharge current, Equations (2) and (3) show that the pulse duration can have a large, though indirect, effect on the PFN mass via its impact on the pulse power and thus on the pulse voltage. In general, these simple scaling rules indicate that PFN mass increases with mission total impulse and thruster specific impulse, and decreases with increasing number of pulses, number of thrusters, thruster efficiency, and discharge voltage.

Detailed assessment of the PFN mass requires a more complete examination of the impacts of PFN design and capacitor characteristics. A code was written which permitted rapid evaluation of the PFN component mass as a function of mission and capacitor characteristics, total number of pulses, thruster performance, pulse duration, and number of PFN stages. The PFN configuration variables considered in the code are illustrated in Fig. 4. The required capacitance and inductance per PFN stage were calculated from:⁴⁶

$$C_s = \frac{\tau_p}{2N_s Z_o} \quad L_s = \frac{\tau_p Z_o}{2N_s} \quad (4)$$

The number of capacitors in series within each PFN stage was calculated by dividing the PFN charging voltage, which is twice the thruster discharge voltage, by the rated capacitor voltage. Resistors required to maintain equal voltages across the series capacitors were included. The number of parallel capacitor sets within a stage was then calculated given the capacitance per stage. The number of extra capacitors needed to ensure adequate PFN lifetime was estimated from the reliability data for each capacitor type, given in percent failure per one thousand hours at a given voltage. This estimate does not account for the lifetime dependence on the number of charge/discharge cycles, because those data were not available for several capacitor types, but rather used the number of total hours of charging time. The number of silicon controlled rectifiers, SCRs, was calculated by dividing the discharge current by the rated current capability of the SCR and adding two to ensure adequate margin. No failure rates were available for the SCRs, so it was not possible to estimate lifetimes. The inductor geometry was a flat spiral. The inductor mass was minimized by varying the spiral geometry while maintaining the required inductance. The code calculated total component masses and PFN power losses during the charge and discharge phases of operation.

Metallized film, both tantalum and aluminum electrolytic, and ceramic capacitors were evaluated. The capacitor designations and characteristics, obtained from vendor catalogs or other published data, are provided in Table 2.⁴⁷⁻⁵⁰ The aluminum electrolytic capacitors were included to illustrate the potential advantages of improved capacitors even though they are not considered suitable for long-term space application due to their poor reliability.⁵⁰ The potential impact of newer double-layer capacitor technology under development at the Space Power Institute of Auburn University⁵¹ is discussed below.

PFN component masses were calculated for a LEO - GEO transfer mission with a velocity increment of 6000 m/s and total impulse of 2.6×10^7 N-s. The mission velocity increment includes a plane change maneuver, and the total impulse was obtained by establishing the spacecraft and mission characteristics as discussed below and then multiplying the time average thrust by the trip time. In addition, it was assumed that two thrusters had to be operating simultaneously, and the thruster efficiency was set to 0.5 for all cases. All other parameters were varied

over a wide range to establish trends in PFN mass. The PFN code was run for MPD thruster specific impulses between 2000 and 6000 seconds, discharge durations between 1.5 and 4 ms, current levels between 5 and 10 kA, and for a total number of pulses between 2×10^8 and 8×10^8 . This number of pulses ranges from a factor of 3 below to 30% above the number for which automobile fuel injectors are currently qualified. These parameter ranges correspond to thruster pulse frequencies from 1 to 30 Hz and peak thrust levels from 20 to 50 N.

Results showed that changing the number of PFN stages from 4 to 8 resulted in less than a 2% change in the PFN component mass. This result justified use of a 4 stage PFN, which has been shown to provide an adequately flat topped pulse on flight systems.⁵² Typical code results for a 4 stage PFN are given in Table 3, in which the number of capacitors and the PFN component masses are provided for a set of two 4000 s I_{sp} thrusters with 50% efficiency and 3×10^8 pulses per thruster. The pulse duration was 2 ms. From Table 3 it is clear that the aluminum electrolytic capacitors, which are the least suitable for long duration space missions, yield the lowest parts count and PFN mass. Next in order of increasing PFN mass are the ceramic, metallized film, and tantalum electrolytic capacitors. For the case shown there is not much difference between the lighter ceramic and the aluminum electrolytic. Note that in both cases the specific mass of the PFN components would be below 5.5 kg/kW for a 10 kW spacecraft. In addition, for all cases the PFN efficiency is over 97%, with approximately one half of the losses occurring across the SCRs.

For almost all discharge current and specific impulse combinations it was possible to find choices of pulse duration and number of pulses for which either the ceramic or metallized film capacitors yielded PFN component masses below 55 kg. This lack of sensitivity to thruster operating condition is important because it is not yet possible to specify the operating conditions for a high performance MPD thruster. However, the PFN mass scaling is not simple because of the coupling between the number of series capacitors, the discharge voltage, and the thruster performance. This coupling is illustrated in Fig. 5, which shows the variation in PFN mass as a function of thruster I_{sp} for the metallized film, Z5U ceramic, and the lighter of the tantalum capacitor types with a constant discharge current of 7.5 kA. Physically this variation in thruster performance would be obtained by varying the number of coils in the applied-field magnet to increase the applied-field strength, and thus the specific impulse, with a constant discharge current. For a given number of capacitors, the PFN mass decreases with increasing specific impulse until the discharge voltage increase forces the addition of another layer of capacitors. These results are not the lowest obtainable PFN component masses because both the discharge duration and number of pulses were held constant for all cases. These data illustrate that a single capacitor type is not optimal for all thruster and mission performance levels. PFN component mass is not sensitive to spacecraft power level, which is accounted for via the heat rejection system mass. Estimates of packaging requirements for flight type power electronics result in a factor of 2 increase in mass over the component masses,⁵³ yielding a constant PFN mass of 110 kg using off-the-shelf capacitor technology. As with the thruster, the PFN thermal control system can be designed for the maximum mission power level, and decreases in power level due to solar array degradation can be accommodated simply by changing the pulse frequency.

High Speed Valve Supply. - Fuel-injector valves require a 12V, 5A square wave of duration equal to the thruster pulse length. A mass allocation of 1 kg was considered conservative for a fuel injector valve supply. The Japanese FAV power supply is combined with a trigger supply for the thruster discharge. Both the FAV and trigger supply are driven by small capacitor discharges and the combined weight of the system is 5 kg.⁵⁰ Based on these data, a mass of 2 kg was used for the valve power supply in this study.

Thermal Management for CCU, PFN, and Cathode Heater Supply

The power system components requiring temperature control are the CCU, PFN, cathode heater supply, and the high-speed valve supply. Requirements for the CCU are very similar to arcjet power processors, and temperature limits will likely be similar. Arcjet power processor baseplate temperatures are currently 50 °C during operation. Similarly, the cathode heater and high-speed supplies will be limited to 50° C. The only components of the PFN requiring temperature control are the capacitors and SCRs, which are typically limited to below 80° C.⁴⁷⁻⁵⁰

Several authors have developed simple ways to estimate thermal control system masses for ion thruster based propulsion systems. Byers³⁷ based his formula on a detailed study of ion propulsion systems by Hawthorne,⁵⁴ and arrived at a specific thermal control system mass of 31 kg/kW of rejected heat for an assumed baseplate temperature of 50° C and a radiator heat rejection of 0.35 kW/m². Hardy³⁶ updated those results to arrive at a specific mass of 27 kg/kW. Later analyses by Brophy and Aston³⁵ distinguished between heat generated by the ion thruster PPU's and the power subsystem, with a specific mass of 20.5 kg/kW for the PPU's and 31.8 kg/kW for the power subsystem thermal control units. They also used a PPU baseplate temperature of 50° C. The power subsystem in their study included the high voltage power distribution unit, the low voltage power distribution unit, the DC/DC converter, and the battery system. Hermel, et al.⁵⁵ used more conservative values of radiator specific mass (11 kg/kW), but did not call out the other elements of the rest of the heat rejection system, so it was impossible to establish a total mass value for this subsystem. More recent studies for both communications and Earth-observing satellites arrived values closer to the 30 kg/kW mentioned above. Price et al.⁵⁶ used a specific mass for thermal control of 29.5 kg/kW for 3-axis stabilized geosynchronous communications satellites and Pidgeon⁵⁷ used a value of 40 kg/kW based on historical data and technology forecasts. However, Pidgeon's analysis was for the entire spacecraft, including heat rejection for the bus, power source, and payload heat rejection, whereas the earlier studies reflected only the requirements of the propulsion system. Based on this review of previous work, a heat rejection system specific mass of 30 kg/kW of heat rejected by all the propulsion power systems was selected.

Propellant Storage and Distribution

Several recent studies have examined the long term storage of cryogenic hydrogen for hydrogen arcjets. A General Dynamics study,⁴¹ building on the capabilities of the Centaur upper stage, found that the tankage fraction for a 200 day LEO - GEO transfer mission was 0.18 including the tank, insulation, and micrometeoroid protection. The single-fault tolerant propellant feed system, including the compressors needed to boost the propellant supply pressure to the required 2.75×10^6 Pa and redundant high-pressure accumulators, weighed 74 kg. The compressors would not be required for the lower pressure pulsed MPD thruster system as the tank pressure of 1×10^5 Pa would be sufficient, and the reduction in feed pressure and flow rate would also reduce the mass of the other propellant feed system components. The tank pressure is maintained at this level throughout the mission by a small heater in the tank. For this study the tankage fraction was kept constant at 0.18 and the mass of the propellant feed system was reduced to 37 kg for the pulsed MPD thrusters. As discussed above, the high-speed valves were included in the thruster component.

The use of deuterium propellant in pulsed MPD thrusters has two potentially large benefits. First, the factor of two increase in propellant storage density will reduce the tankage fraction to 0.09. Second, the tank volume will also be reduced by a factor of approximately two, which could mitigate the need for a new launch vehicle fairing required for hydrogen arcjets.⁴¹ Of course, the new fairing may not be required with hydrogen propellant either, because the higher specific impulses associated with MPD thrusters greatly reduces propellant requirements compared to arcjets.

Pulsed System Integration Issues

Many pulsed electromagnetic propulsion systems with peak powers between 1 and 3 MW have been flown both operationally and as experiments.^{9,10} Qualification of these systems has required evaluation of structural interfaces, electromagnetic interference, plume property distributions, spacecraft contamination, and thermal loads. The most important of these which are relevant to pulsed MPD thruster systems are EMI and plume property distributions, where the latter are a concern due to the potential impact on communication signals. EMI has been extensively studied in this country for 2 - 3 MW peak power, microsecond duration, pulsed-plasma thrusters and by the Japanese for pulsed MPD thrusters.^{6,7,9-11} Potential issues were identified in both cases which were corrected via simple modifications of the power system. Minor interference resulting from the firing of the pulsed plasma thruster on the NOVA I spacecraft was eliminated on NOVA II and III.¹⁰ Plume property distributions for pulsed MPD thrusters

are not well known for distances beyond 30 cm from the exit plane, so it is not possible to comment quantitatively on their impact on communication signals. However, no issues of this type were reported on the MS-T4 flight of an ammonia applied-field thruster.⁵

Propulsion System Comparison

A simple model was written to quantify the mission trades associated with using a pulsed MPD thruster system and to compare the results with those attainable using hydrogen arcjets. A LEO - GEO transfer mission including a plane change, with a total velocity increment of 6000 m/s, was analyzed for payloads between 1000 kg and 2000 kg and spacecraft power levels between 10 and 40 kW. These values were chosen to span the range of other studies using hydrogen arcjets and to examine the power - I_{sp} trade-offs of LEO - GEO transfer missions. The effects of eclipse and drag were not explicitly included in this study. Hermel et al.⁵⁵ found that approximately 9% of a low thrust LEO - GEO transfer would be spent in eclipse resulting in a corresponding increase in trip time. While drag was not explicitly included in this study, the 370 km initial altitude did not significantly penalize a 30 kW SEOTV studied by General Dynamics.⁴¹

A summary of the pulsed MPD thruster and hydrogen arcjet system masses is given in Table 4. Two thrusters were assumed to be operating simultaneously for spacecraft control. Six hydrogen arcjets, each with a single string power processing unit, were assumed based on an expected thruster lifetime of 1750 hr.⁴¹ As discussed above, the lower power, temperatures, and current densities present in the pulsed MPD thruster yield an expected lifetime of 5000 hrs, resulting in a requirement of four MPD thrusters for a 200 day mission. This allows for failure of two of the thrusters without affecting the mission. Single-string propulsion systems were assumed, so that each thruster had a complete set of the power supplies shown in Fig. 1. The same PFN and MPD thruster masses were used for the entire power range, with power scaling accomplished by changing the pulse frequency.

The final spacecraft mass was calculated for both the hydrogen arcjet and pulsed MPD thruster cases by solving the rocket equation for the final mass, M_f , in terms of all the known spacecraft masses, the mission velocity change and thruster specific impulse, and the tankage fraction. A five percent propellant contingency was added and the result increased by 30% for additional contingency. The result was:

$$M_f = \frac{1.3 \times (M_{p.s.} + M_{pow} + M_{p.c.} + M_{str} + M_{pay})}{\left\{ 1 - [1.05T_f + 0.05] \left[\exp\left(\frac{\Delta V}{I_{sp}g_o}\right) - 1 \right] \right\}} \quad (5)$$

where $M_{p.s.}$ is the propulsion system mass which includes all the power supplies needed for all thrusters, M_{pow} is the power system mass which includes the arrays and their deployment and control mechanism, and $M_{p.c.}$ is the propellant management system mass which includes all the all tank utilities. The initial spacecraft mass in low earth orbit (IMLEO) was calculated using the result for M_f and reapplying the rocket equation. Trip time was evaluated by dividing the propellant mass by the total propellant flow rate, where the latter was obtained from the flow rate to each thruster:

$$\dot{m} = \frac{2\eta_t P_t}{I_{sp}^2 g_o^2} \quad (6)$$

and multiplying the result by the number of thrusters in operation. In this equation P_t is the power actually delivered to the thruster, which accounts for both CCU and PFN losses. For the pulsed thrusters P_t is equal to P_p , and Equation (6) yields the peak flow rate during the pulse. This was rescaled to the average flow rate by

multiplying by the pulse duration and the pulse frequency.

For this study the hydrogen arcjet performance was set to 1200 s I_{sp} at 45% efficiency,⁴¹ values which overestimate the capabilities of current arcjets. Based on the recent results from Princeton¹⁶ and Japan,¹⁷ the MPD thruster efficiency was set to 50% and the specific impulse was varied between one and five times the arcjet specific impulse. While this may overestimate the performance of the MPD thruster at low specific impulses, there has not been sufficient study of pulsed H_2 or D_2 applied-field MPD thrusters to establish optimum performance levels. A 370 km initial orbital altitude was used based on the General Dynamics SEOTV study.⁴¹

Figure 6 shows IMLEO for 10, 20, 30, and 40 kW spacecraft with a 1000 kg payload for both hydrogen arcjets and pulsed MPD thrusters. The payload capabilities of four launch vehicles to the 370 km initial orbit are also shown.^{41,58} The IMLEO for the hydrogen arcjet based systems are 4350, 5250, 6140, and 7040 kg for the 10, 20, 30, and 40 kW power levels, respectively. The mass benefits of the higher I_{sp} pulsed MPD thruster are clearly evident for all power levels. As expected, for equal values of I_{sp} the pulsed system penalizes the spacecraft mass when compared to the H_2 arcjet system, resulting in mass increases of about 800 kg for a 10 kW spacecraft. These penalties, which result from the 110 kg PFN mass and the assumed single-string system approach, force an increase in launch vehicle class for a 1200 s I_{sp} pulsed MPD thruster. However, the advantages of the pulsed MPD thruster are clear for higher specific impulses. The spacecraft IMLEO decreases rapidly with increasing specific impulse and asymptotes to approximately 3200, 3700, 4200, and 4800 kg for the 10, 20, 30 and 40 kW spacecraft, respectively. These values reflect IMLEO reductions of up to 3000 kg for specific impulses above 4000 s. The spacecraft mass breakdown for the 40 kW, 4000 s I_{sp} hydrogen pulsed MPD thruster propelled spacecraft, using subsystems as defined in Eqn. (5), is given in Table 5. The table shows that, for this example, the highest leverage technologies are the spacecraft power and propulsion systems. As is clear from Fig. 6, the mass savings resulting from use of higher I_{sp} pulsed MPD thrusters can be used to reduce the launch vehicle class. Increasing the I_{sp} to approximately 2000 s permits use of a smaller launch vehicle for every power level studied, and for most cases increasing I_{sp} to over 2100 s allows a further launch vehicle class reduction. For example, the 20 kW pulsed MPD thruster operating at 1200 s I_{sp} would require an Atlas IIA launch vehicle, but increasing the I_{sp} to 2200 s allows use of a Delta 7920. The 20 kW arcjet system would require an Atlas I vehicle. The 40 kW pulsed MPD thruster spacecraft at 1200 s I_{sp} could not be launched on the Atlas IIAS, but if operated at 3000 s it could use an Atlas I, and at 4000 s I_{sp} it could be launched on a Delta 7920. A 40 kW H_2 arcjet requires an Atlas IIAS for launch.

Of course, as shown in Fig. 7, there are trip time penalties associated with the higher specific impulses. For equal values of I_{sp} , the two propulsion systems accomplish the LEO - GEO transfer in about the same time, and the pulsed MPD thruster system trip time increases approximately linearly with I_{sp} . At a power level of 10 kW neither H_2 arcjets nor pulsed MPD thrusters can accomplish the orbit transfer in less than 330 days. For higher power levels both the absolute magnitude of the trip time and its rate of increase with I_{sp} decrease rapidly, reaching a minimum value of 130 days at 40 kW and 1200 s I_{sp} . The 40 kW system trip time achieves a trip time of 300 days at an I_{sp} of 4000 s. For cases in which the launch vehicle is fixed by other constraints the propulsion system trade-offs are only between trip time and power level. For example, from Fig. 6 it is seen that if the launch vehicle is constrained to a Delta 7920 the maximum arcjet power level is approximately 10 kW with a trip time of 330 days. The pulsed MPD thruster would require specific impulses of 2000, 3000, and 4000 s for power levels of 20, 30, and 40 kW, respectively, for launch on the Delta 7920. The corresponding trip times are 260, 280, and 300 days, yielding trip time savings of 70, 50, and 30 days over that achieved with the H_2 arcjet.

These propulsion system trade-off trends are duplicated for a heavier 2000 kg payload. As shown in Figures 8 and 9 for spacecraft power levels of 20 and 40 kW, the heavier spacecraft reduces the penalty associated with using a low I_{sp} pulsed MPD thruster system and precludes use of the Delta 7920. The reduced mass penalty at low I_{sp} is

due to the smaller propulsion system mass fraction for the higher total spacecraft masses. For the heavier payload neither the H_2 arcjet nor the pulsed MPD thruster can be launched on an Atlas IIAS, and there is almost no launch margin with the 30 kW H_2 arcjet system. For an I_{sp} of 2300 s a 30 kW pulsed MPD thruster system can be launched on an Atlas IIA, and at 4000 s I_{sp} it can be launched on an Atlas I. Use of a 40 kW, 3600 s I_{sp} , pulsed MPD thruster permits use of an Atlas IIA with a trip time of 300 days. To achieve a trip time lower than 200 days using a single string propulsion system having a 110 kg PFN, either the specific impulse must be below 2000 s or the spacecraft power must be increased over 40 kW.

The impacts of improved PFN technology and the use of deuterium propellant were examined by reducing the PFN mass to a constant 55 kg and reducing the tankage fraction to 0.09. No other changes were made. As discussed above, the power system mass is a dominant element of pulsed thruster systems, and PFN mass reduction would require use of advanced capacitor technologies such as those being developed at the Space Power Institute of Auburn University⁵¹ and the Lawrence Livermore National Laboratory.⁵⁹ A principal benefit of the use of deuterium propellant would be the volume reduction of the propellant tank and its impact on launch vehicle payload fairing requirements. IMLEO reduction and trip time estimates resulting from use of a 55 kg PFN are shown in Figs. 10 and 11 for a 1000 kg payload and 40 kW spacecraft, from which it is seen that the lower PFN mass eliminates almost all of the mass penalty at low values of I_{sp} , and reduces the trip time by between 10 and 25 days for missions lasting less than one year. The effect of using deuterium propellant and of combining the use of D_2 with a low mass PFN on IMLEO reduction are shown in Fig. 12. As with the PFN mass reduction, using D_2 propellant eliminates the mass penalty associated with operating the pulsed MPD thruster at the same I_{sp} as the H_2 arcjet, but the benefit of D_2 decreases with increasing I_{sp} because of the reduction in propellant mass. The combined use of D_2 propellant and an advanced technology PFN results in a lower system mass for the pulsed MPD thruster for all values of I_{sp} , and would permit use of a Delta 7920 launch vehicle with a 40 kW spacecraft using a thruster having 3000 s I_{sp} . Figure 13 shows that, for a given specific impulse, the advanced technologies result in a 20 day decrease in trip time for a given I_{sp} . More dramatic, however, is the effect on the trip time for a given launch vehicle. As discussed above, for the H_2 arcjet to be launched on a Delta 7920 the power level must be decreased to approximately 10 kW with an associated trip time of 330 days. A pulsed MPD thruster system using D_2 propellant with a 55 kg PFN operating at 3000 s specific impulse could also be launched on a Delta 7920, but the trip time is only 200 days. This result clearly shows that large benefits result from using D_2 and reducing the PFN mass. No attempt was made to quantify the potentially dominant benefits of D_2 propellant usage resulting from the propellant tank volume reduction.

Conclusions

The system requirements for pulsed MPD thruster based solar-electric orbit transfer vehicles were studied to establish the component and spacecraft masses for LEO - GEO transfer missions at power levels from 10 to 40 kW. Potential benefits of pulsed MPD thrusters over alternative electric propulsion concepts include ease of power scaling required by array degradation or increased distance from the sun, improved transportability from low power flight tests to operational vehicles, and reduced in ground qualification costs. In addition to the thruster and propellant management system, a pulsed MPD thruster propulsion system requires a charge control unit, a pulse forming network, a cathode heater supply, and a high speed valve supply. Propellant efficiencies greater than 98% appear achievable via careful design of the propellant injection system and use of either automobile fuel-injector valve or the Japanese Fast Acting Valve technologies. Fuel injector valves are routinely qualified for 6×10^8 pulses, which is between 2 and 3 times the number of pulses required for a LEO-GEO transfer mission. The pulse forming network charge control unit appears similar in specific mass characteristics to arcjet power processing units. Off-the-shelf

capacitors can yield pulse forming networks sufficiently small so that the reduction in propellant mass resulting from the higher specific impulses available from MPD thrusters more than offsets the additional power system mass.

A system comparison with hydrogen arcjets using 1000 and 2000 kg payloads revealed that the initial mass in low Earth orbit can be reduced by between 1200 and 3000 kg by using pulsed applied-field MPD thrusters with specific impulses between 2000 and 4500 s and power levels between 10 and 40 kW. The resulting mass and volume reductions can be used to reduce launch vehicle class with an associated reduction in launch cost. There is an increase in trip time with specific impulse which may be acceptable for certain missions. For situations in which the launch vehicle selection is determined by other constraints, use of a higher power, higher specific impulse, pulsed MPD thruster system can result in significant trip time savings. Use of more advanced capacitor technologies and/or deuterium propellant further reduce launch mass and trip time, potentially yielding a 130 day trip time reduction for 1000 kg payload launched on a Delta 7920. In addition, use of deuterium greatly reduces the propellant volume and may eliminate the need for larger launch vehicle payload shrouds. The potential system, mass, volume, and cost benefits indicate that pulsed MPD thrusters are an attractive option for orbit transfer vehicles.

References

1. Myers, R.M., Mantenieks, M.A., and LaPointe, M.R., "MPD Thruster Technology," AIAA Paper 91-3568, Sept. 1991, see also NASA TM 105242.
2. Sovey, J.S. and Mantenieks, M.A., "Performance and Lifetime Assessment of MPD Arc Thruster Technology," *Journal of Propulsion and Power*, Vol. 7, No. 1, Jan. - Feb. 1991, pp. 71 - 83.
3. Seikel, G.R., York, T.M., and Condit, W.C., "Applied-Field Magnetoplasma Dynamic Thrusters for Orbit-Raising Missions, *Orbit-Raising and Maneuvering Propulsion: Research Status and Needs*, L. Caveny, ed., Prog. in Aeronautics and Astronautics Vol. 89, American Inst. of Aeronautics and Astronautics, New York, 1984, pp. 260 - 286.
4. Polk, J.E. and Pivorotto, T.J., "Alkali Metal Propellants for MPD Thrusters," AIAA Paper 91-3572, Sept. 1991.
5. Kuriki, K., Nakamura, K., and Morimoto, S., "MPD Thruster Test on Engineering Test Satellite," AIAA Paper 79-2071, Oct. 1979.
6. Kuriki, K., "The MPD Thruster Test on the Space Shuttle," *Journal of Spacecraft and Rockets*, Vol. 16, No. 5, Sept. - Oct. 1979, pp. 326-332.
7. Kuriki, K., Kawashima, N., Sazaki, S., Yanagisawa, M., and Obayashi, T., "Space Experiments with Particle Accelerators (SEPAC) Performed in Spacelab First," AIAA Paper 85-1996, Sept. 1985.
8. Sazaki, S., Kawashima, N., Kuriki, K., Yanagisawa, M., and Obayashi, T., "Vehicle Charging Observed in SEPAC Spacelab - 1 Experiment," *Journal of Spacecraft and Rockets*, Vol. 23, No. 2, March - April 1986, pp. 194-199.
9. Myers, R.M., "Electromagnetic Propulsion for Spacecraft," AIAA Paper 93-1086, Feb. 1993.
10. Ebert, W.L., Kowal, S.J., and Sloan, R.F., "Operational NOVA Spacecraft Teflon Pulsed Plasma Thruster System," AIAA Paper 89-2497, July 1989.
11. Shimizu, Y., Toki, K., Suzuki, H., Uematsu, K., Otsuka, T., Shiina, K., and Kunii, Y., "Development of MPD

Arcjet System EM for SFU-1," IEPC Paper 91-147, *Proceedings of the 22nd International Electric Propulsion Conf.*, Viareggio, Italy, Oct. 1991.

12. King, D.Q., "100 kWe MPD Thruster System Design," AIAA Paper 82-1897, Nov. 1982.

13. Rudolph, L.K., "Design and Benefits of Pulsed MPD Thruster Orbit Transfer Vehicles," IEPC Paper 84-81, *Proceedings of the 17th International Electric Propulsion Conf.*, Tokyo, Japan, May 1984.

14. Polk, J.E., Kelly, A.J., and Jahn, R.G., "Characterization of Cold Cathode Erosion Processes," IEPC Paper 88-075, *Proceedings of the 20th International Electric Propulsion Conference*, Garmish-Partenkirchen, Germany, Oct. 1988.

15. Taylor, R.D., Burton, R.L., and Wetzell, K.K., "Preliminary Investigation of a Low Power Pulsed Arcjet Thruster," AIAA 92-3113, July 1992.

16. Miller, G.E. and Kelly, A.J., "Hydrogen Performance Measurements," in Electric Propulsion Laboratory Progress Report MAE 1776.38, Princeton University, Dept. of Mechanical and Aerospace Engineering, July - Aug. 1992.

17. Tahara, H., Sazaki, M., Kagaya, Y., and Yoshikawa, T., "Thruster Performance and Acceleration Mechanisms of a Quasi-steady Applied-field MPD Arcjet," AIAA Paper 90-2554, July 1990.

18. Schoenberg, K., Gerwin, R., Henins, I., Mayo, R., Scheuer, J., and Wurden, G., "Preliminary Investigation of Power Flow and Electrode Phenomena in a Multi-Megawatt Coaxial Plasma Thruster," NASA CR 191084, March 1993.

19. Mikellides, P. and Turchi, P.J., "Application of the MACH2 Code to Magnetoplasmdynamic Arcjets," AIAA Paper 92-3740, July 1992.

20. Shroff, A.M., Palluel, P., and Tonnerre, J.C., "Performance and Life Tests of Various Types of Impregnated Cathodes," *Applications of Surface Science*, Vol. 8, North Holland Publ., 1981, pp. 36 - 49.

21. Forrest, S.M., Green, M.C., Herrmannsfeldt, W.B., and Palmer, R.B., "A Bombarder Heated Reservoir Cathode for a 36 A/cm² Hour Life Application," Varian Electron Device Business Unit, Presented at the 1992 Tri-Service/NASA Cathode Workshop, Greenbelt, Md, March 1992.

22. Slutz, R. J., "A 10,000-hr Life Test of an Engineering Model Resistojet," NASA TM 103216, Oct. 1990.

23. Gallimore, A.D., Kelly, A.J., and Jahn, R.G., "Anode Power Deposition in Quasisteady Magnetoplasmdynamic Thrusters," *Journal of Propulsion and Power*, Vol. 8, No. 6, Nov. - Dec. 1992, pp. 1224 - 1231.

24. Myers, R. M., "Applied-Field MPD Thruster Geometry Effects," AIAA 91-2342, June 1991; See also NASA CR 187163.

25. Yoshikawa, T., Kagaya, Y., and Tahara, H., "Continuous Operational Tests of a Quasi-Steady MPD Arcjet System," IEPC Paper 91-075, *Proceedings of the 22nd Intern. Electric Propulsion Conference*, Viareggio, Italy, Oct. 1991.

26. Mantenieks, M.A. and Myers, R.M., "100-kW Class Applied-Field MPD Thruster Component Wear," 10th Symp. on Space Nuclear Power and Propulsion," *AIP Proceedings No. 271*, Jan. 1993, pp. 1317-1326, see also

27. Palumbo, D.J., "Solid Propellant Pulsed Plasma Propulsion System Development for N-S Stationkeeping," AIAA Paper 79-2097, Oct. 1979.
28. Tahara, H., Kagaya, Y., and Yoshikawa, T., "Hybrid MPD Thruster with Axial and Cusp Magnetic Fields," IEPC Paper 88-058, *Proceedings of the 20th Intern. Electric Propulsion Conf.*, Garmish-Partenkirchen, Germany, Oct. 1988.
29. Yoshikawa, T., Kagaya, Y., Tahara, H., and Wasa, T., "Continuous Operation of a Quasi-steady MPD Thruster Propulsion System with an External Magnetic Field," IEPC Paper 88-056, *Proceedings of the 20th Intern. Electric Propulsion Conf.*, Garmish-Partenkirchen, Germany, Oct. 1988.
30. LaPointe, M.R., private communication, NASA Lewis Research Center, Cleveland, OH, 1993.
31. Jones, R.M., "Propellant Injection for MPD Thrusters," AIAA 79-2074, Oct. 1979.
32. Suzuki, H., Uematsu, K., Ohtsuka, T., Shiina, K., Toki, K., and Shimizu, Y., "3 Million Shots Endurance Test of 1 kW Class Arcjet Thruster," IEPC Paper 88-014, *Proceedings the 20th Intern. Electric Propulsion Conf.*, Garmish-Partenkirchen, Germany, Oct. 1988.
33. Bordewyka, T., personal communication, A.C. Rochester, Grand Rapids, MI, March 1993.
34. Rosenthal, R., Grethen, D., and Kriebel, M., "Design Integration of Electric Propulsion Systems," AIAA 93-1083, Feb. 1993.
35. Brophy, J.R. and Aston, G., "A Detailed Model of Ion Propulsion Systems," AIAA 89-2268, July 1989.
36. Hardy, T.L., Rawlin, V.K., and Patterson, M.J., "Electric Propulsion Options for the SP-100 Reference Mission," *Proc. of the 4th Symposium on Space Nuclear Power Systems*, The Institute for Space Nuclear Power Studies, Albuquerque, NM, Jan. 1987.
37. Byers, D.C., Terdan, F.F., and Myers, I.T., "Primary Electric Propulsion for Future Space Missions" NASA TM 79141, May 1979.
38. Sarver-Verhey, T.R., "Extended Testing of Xenon Ion Thruster Hollow Cathodes," AIAA Paper 92-3204, July 1992, see also NASA CR 189227.
39. Stella, P.M. and Kurtland, R.M., "Development Testing of the Advanced Photovoltaic Solar Array, *Proc. of 26th IECEC*, Vol. 2, Aug. 1991, p. 269-274.
40. Stella, P.M. and Flood, D., "Photovoltaic Options for Solar Electric Propulsion," AIAA Paper 90-2529, July 1990.
41. Anon., "Feasibility of Applying Centaur Technology to an EOTV Propellant Storage and Management System, Final Presentation," General Dynamics, Space Systems Division, Contract NAS3-25972, Task Order No. 7, NASA Lewis Research Center, July 31, 1992.
42. Caldwell, D.J., "System Design of ELITE Power Processing Unit," *Proc. of 26th Intersociety Energy Conversion Engineering Conf. (IECEC)*, Aug. 4, 1991, p. 174-179.

43. Patterson, M., et al., "Plasma Contactor Technology for Space Station Freedom," Proposed AIAA Paper 93-2228, June 1993.
44. Beattie, J.R., Robson, R.R., and Williams, J.D., "18-mN Xenon Ion Propulsion Subsystem," IEPC Paper 91-010, *Proceedings of the 22nd International Electric Propulsion Conf.*, Viareggio, Italy, Oct. 1991.
45. Lovell, M. "The UK-10 Power Conditioning and Control Equipment," AIAA Paper 90-2631, July 1990.
46. Humphries, S. Jr., *Principles of Charged Particle Acceleration*, John Wiley and Sons, New York, 1986, pp. 254 - 262.
47. AVX Corporation, Ceramic Advanced Products, Cincinnati, OH 45211, 1993.
48. Sprague, Tantalum Capacitor Catalog, Stanford, Maine, 04073. 1993.
49. Mallory Capacitor Co., Electronic Components General Catalog, Indianapolis, Indiana 46241, 1993.
50. Kunii, Y., et al., "Verification of Performance and Endurance of Capacitor Bank for the Electric Propulsion Experiment," IEPC Paper 88-048, *Proceedings of the 20th Intern. Electric Propulsion Conf.*, Garmish-Partenkirchen, Germany, Oct. 1988.
51. Rose, M.F., Private Communication, University of Auburn, Space Power Institute, Dec. 1992.
52. Toki, K., Shimizu, Y., Kuriki, K., Suzuki, H., and Kunii, Y., "The MPD Arcjet Thruster System for Electric Propulsion Experiment Onboard Space Flyer Unit," *Proc. of the 17th International Symp. on Space Technology and Science*, Tokyo, Japan 1990.
53. Anon., "30-Centimeter Ion Thrust Subsystem Design Manual," NASA TM-79191, June 1979.
54. Hawthorne, E.I., et al., "Extended Performance Solar Electric Propulsion Thrust System Study, Vol. III, Trade-off Studies of Alternate Thrust System Configurations," Hughes Research Labs., Malibu, Calif. and Hughes Space and Communications Group, Los Angeles, CA, Sept. 1977, see also NASA CR-135281.
55. Hermel, J., Meese, R.A., Rogers, W.P., Kushida, R.O., Beattie, J.R., and Hyman, J., "Modular, Ion-Propelled, Orbit-Transfer Vehicle," *Journal of Spacecraft and Rockets*, Vol. 25, No. 5, Sept.-Oct. 1988.
56. Price, K.M., Pidgeon, D.J., and Tsao, A., "Mass and Power Modeling of Communications Satellites, NASA CR 189186, Dec. 1991.
57. Pidgeon, D.J., "A Subsystem Design Study of an Earth Sciences Geostationary Platform," M.S. Thesis, School of Engineering and Applied Sciences, The George Washington University, July 1989.
58. Anon., "Launch Vehicles Summary for JPL Missions," NASA JPL D6936, Rev. B, March 1992.
59. Mayer, S.T., Pekala, R.W., and Kaschmitter, J.L., "The Aerocapacitor: An Electrochemical Double-Layer Energy Storage Device," *J. Electrochem. Soc.*, Vol. 140, No. 2, Feb. 1993, pp. 446 - 451.

Component	Mass, kg
Anode (Mo)	4.4
Cathode (W)	2
Backplate/insulator (Al ₂ O ₃)	1
Applied-field coil (Cu)	1.8
High speed valve	0.2
Contingency (20% of total)	1.9
Total	11.3

Table 1 - 40 kW applied-field thruster mass breakdown

Capacitor Type (Ref.)	Capacitance (μ F)	Rated Voltage (V)	Mass (kg)	Specific Energy (J/kg)
Metallized film (51)	142	336	0.173	46
Ceramic (48) Z5U	460	200	0.183	50.3
X7R	45	500	0.183	30.7
Tantalum (49) 81F	39	125	0.018	16.9
112	28	200	0.025	22.4
Aluminum (50) CG	3000	250	0.95	98.7
LP	680	250	0.454	46.8

Table 2 - Capacitor characteristics used for PFN optimization.

Capacitor Type	Number of Capacitors	PFN Component Mass, kg
Metallized Film	209	42.5
Ceramic Z5U	257	53.4
Ceramic X7R	657	126
Tantalum 81F	6802	129
Tantalum 112	4214	111
Aluminum CG	41	45.3
Aluminum LP	177	87

Table 3 - Typical results for PFN capacitor requirements and component masses for a LEO - GEO transfer mission. 4000 s Isp, 50% efficiency, and 3×10^8 pulses per thruster.

Component (Ref.)	H ₂ Arcjet	Pulsed H ₂ MPDT	Pulsed D ₂ MPDT
Tankage Fraction (41)	0.18	0.18	0.09
Propellant Feed System (41)	74 kg	37 kg	37 kg
Tank/Feed Venting (41)	46 kg	46 kg	46 kg
Prop. Fill/Drain (41)	5 kg	5 kg	5 kg
Boil-Off Control (41)	20 kg	20 kg	20 kg
Thrusters	0.5 kg/kW	0.3 kg/kW	0.3 kg/kW
Thruster Mounting Str. (37)	0.15 kg/kW	0.09 kg/kW	0.09 kg/kW
Gimbals (37)	0.20 kg/kW	0.12 kg/kW	0.12 kg/kW
Attitude Control Syst. (41)	125 kg	125 kg	125 kg
Solar Arrays (12)	12 kg/kW	12 kg/kW	12 kg/kW
Solar Array Control (41)	5.6 kg/kW	5.6 kg/kW	5.6 kg/kW
Power Processing Unit (42)	3 kg/kW	—	—
Charge Control Unit	—	3 kg/kW	3 kg/kW
High-Speed Valve Supply	—	2 kg	2 kg
Cathode Heater Supply	—	3 kg	3 kg
Pulse-Forming Network	—	110 kg	110 kg
Thermal Management (37,65)	30 kg/kW	30 kg/kW	30 kg/kW

Table 4 - Spacecraft mass breakdown for LEO - GEO transfer missions using H₂ arcjets and H₂ and D₂ pulsed MPD thrusters for power levels between 10 and 40 kW. Five percent propellant contingency and thirty percent mass contingency added to all systems.

Subsystem	Mass, kg
Propulsion, $M_{p.s.}$	955
Power, M_{pow}	704
Propellant control, $M_{p.c}$	270
Structure, M_{str}	100
Tank	124
Payload, M_{pay}	1000
Subtotal	3153
30% contingency	946
Propellant	693
Total IMLEO	4790

Table 5 - Mass breakdown for an 40 kW SEOTV using a 4000 s I_{sp} hydrogen pulsed MPD thruster with current technology capacitors. This spacecraft carries a 1000 kg payload, has a trip time of 300 days, and could be launched on an Delta 7920.

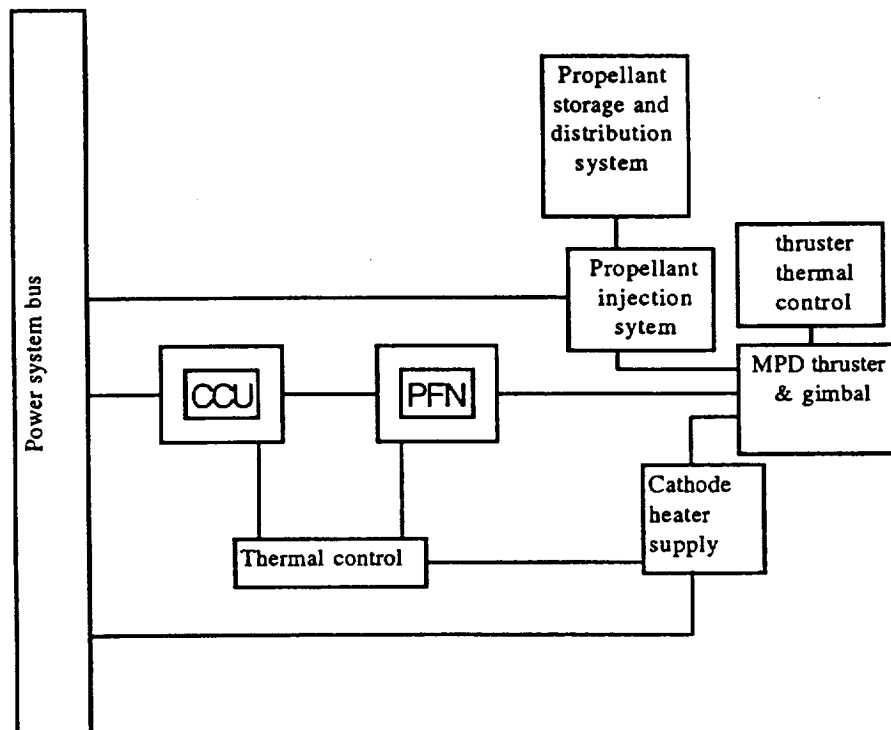


Fig. 1 - Pulsed MPD thruster propulsion system schematic.

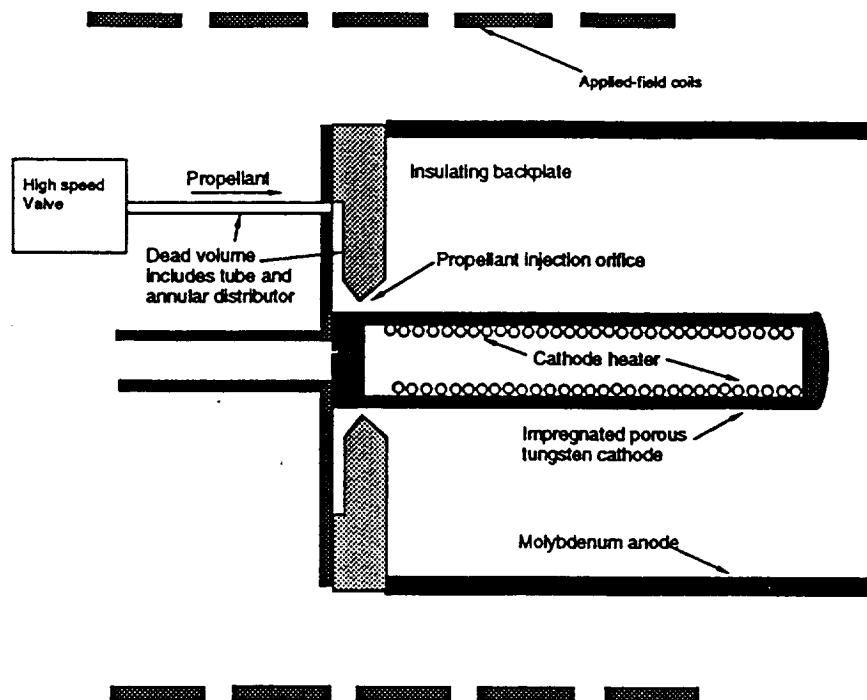


Fig. 2 - Schematic of pulsed applied-field MPD thruster with heated cathode. Not to scale.

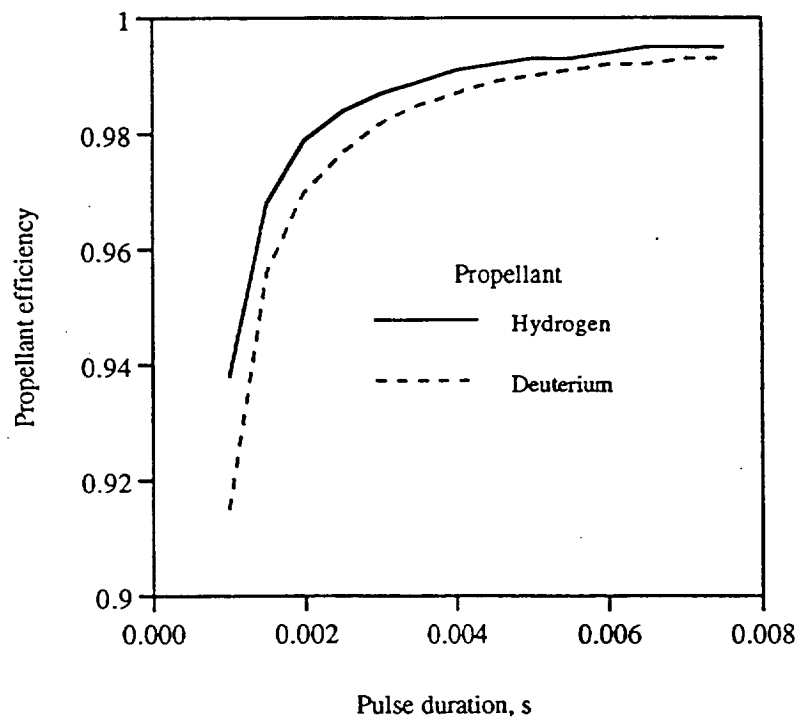


Fig. 3 - Propellant efficiency as a function of pulse duration for two propellants. 0.5 g/s peak flow rate, 6.16 cm³ dead volume, 1.1 x 10⁻⁴ m² orifice area.

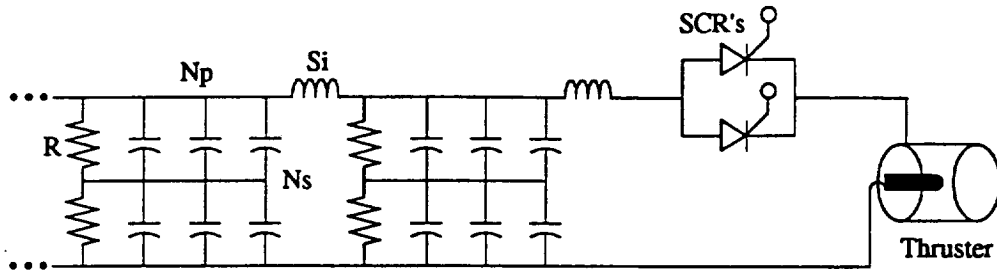


Fig. 4 - PFN schematic showing variable number of series (Ns) and parallel (Np) capacitors, inductor size (Si), resistors (R), and number of silicon controlled rectifiers (SCRs).

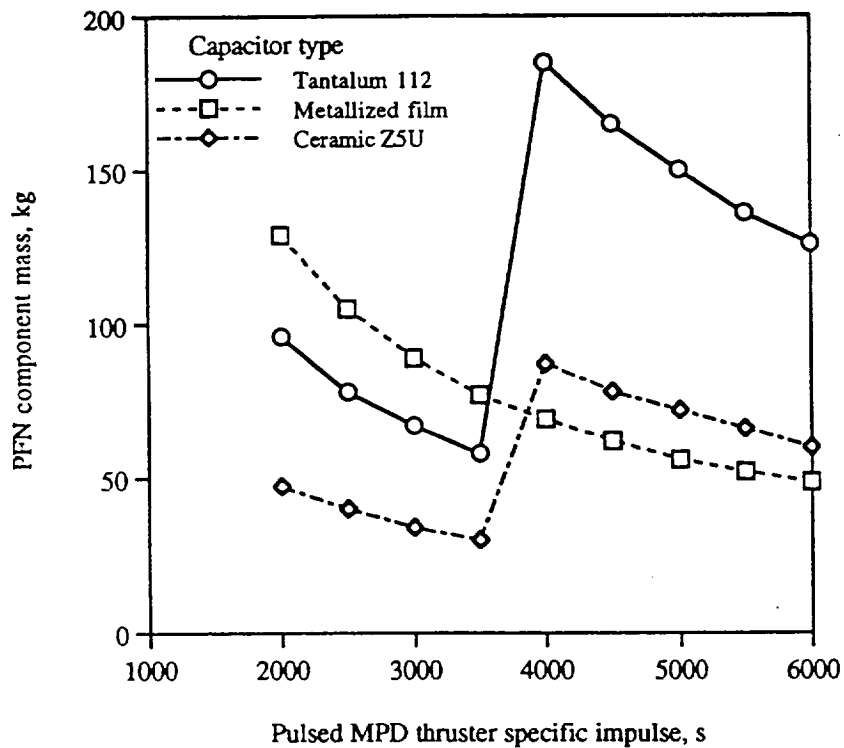


Fig. 5 - Unoptimized PFN component mass variation with thruster specific impulse for 3 capacitor types. LEO - GEO transfer, pulse duration 1.5 ms, 4×10^8 pulses per thruster.

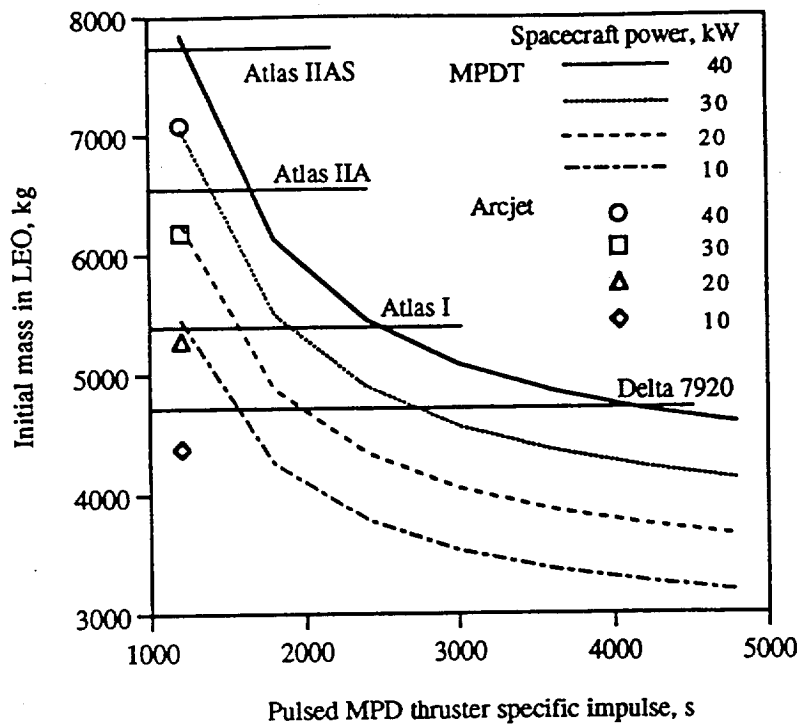


Fig. 6 - Initial SEOTV mass in LEO vs. pulsed MPD thruster specific impulse for four spacecraft power levels. 1000 kg payload, LEO - GEO transfer mission.

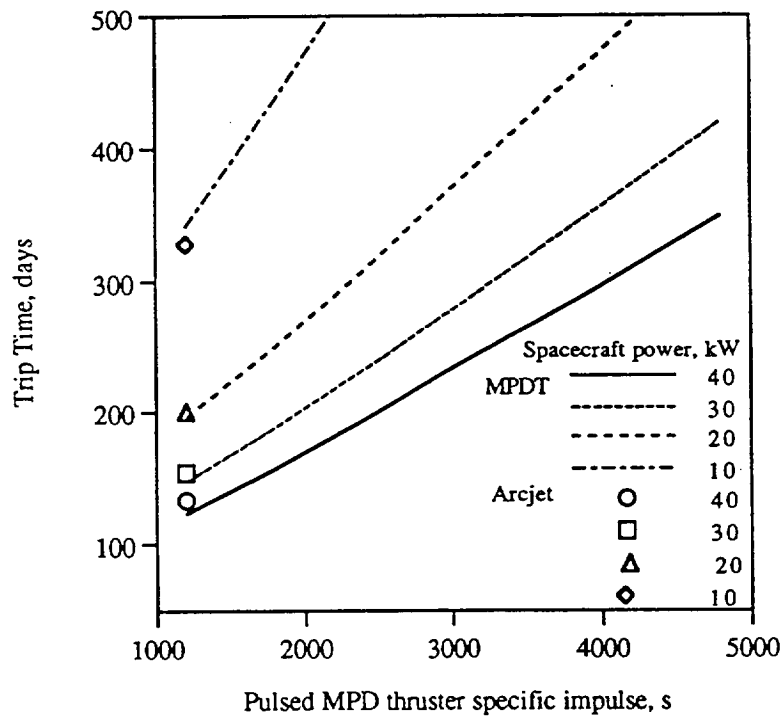


Fig. 7 - Trip time as a function of pulsed MPD thruster specific impulse. 1000 kg payload, LEO - GEO transfer mission

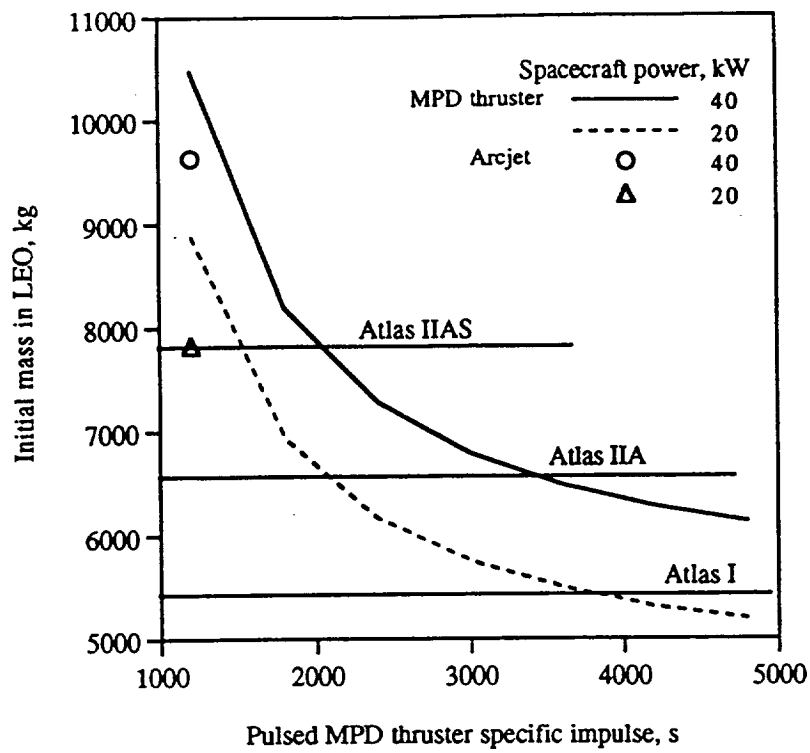


Fig. 8 - Initial mass in LEO vs. pulsed MPD thruster specific impulse for 20 and 40 kW spacecraft. 2000 kg payload, LEO-GEO transfer mission.

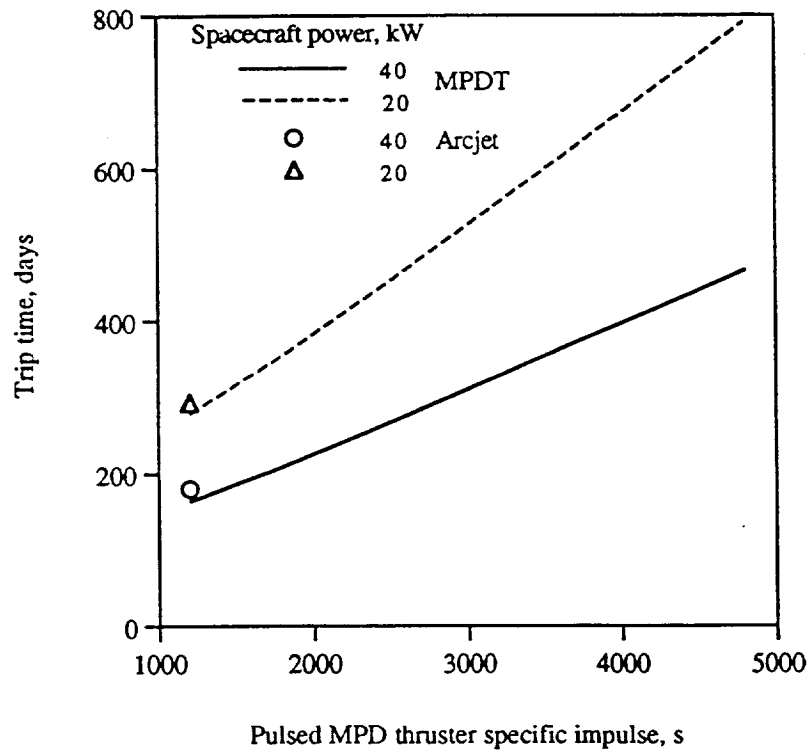


Fig. 9 - Trip time as a function of pulsed MPD thruster specific impulse. 2000 kg payload, LEO - GEO transfer mission.

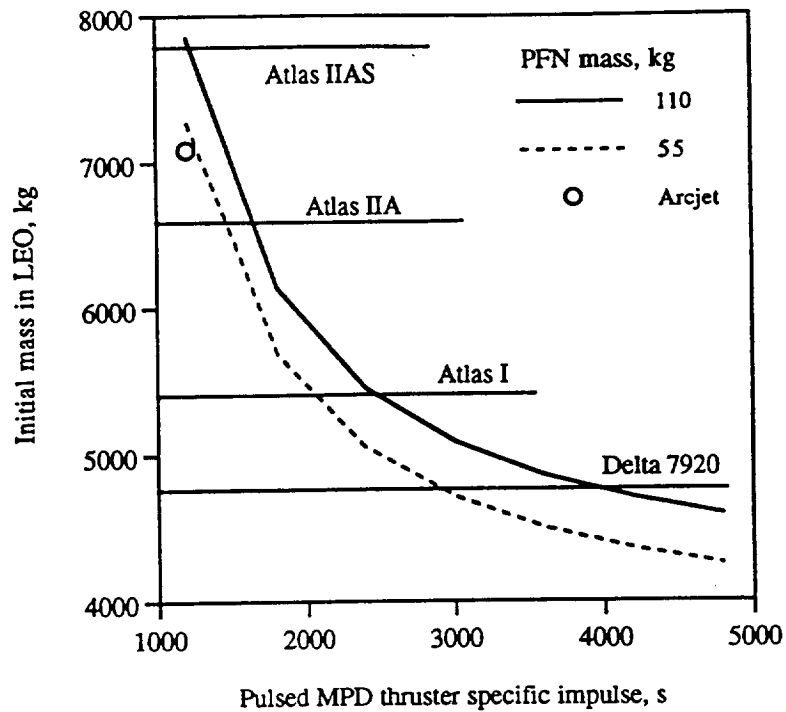


Fig. 10 - Effect of PFN mass on initial mass in LEO vs pulsed MPD thruster specific impulse. 1000 kg payload, 40 kW spacecraft.

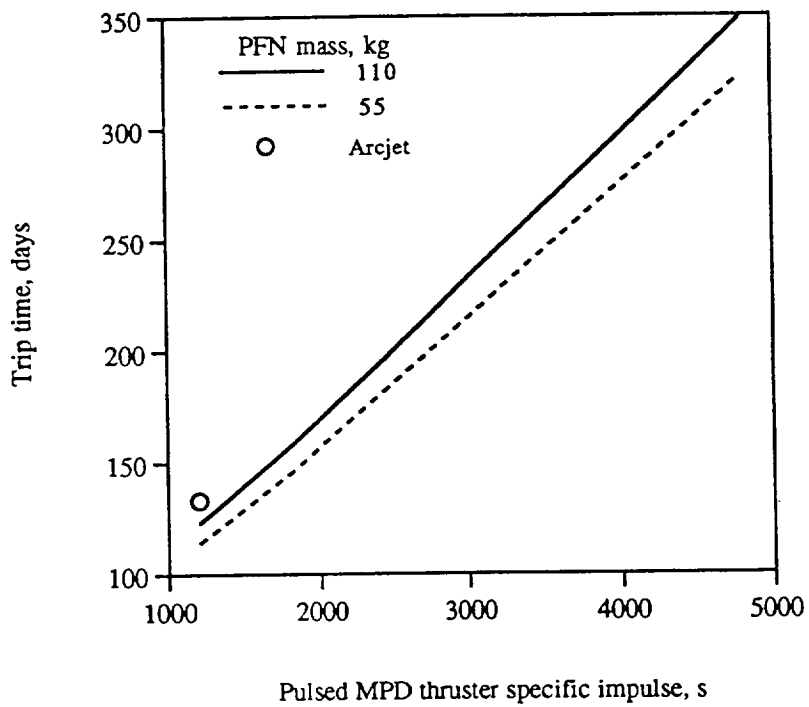


Fig. 11 - Effect of PFN mass on trip time for a 40 kW spacecraft. 1000 kg payload, LEO - GEO transfer mission.

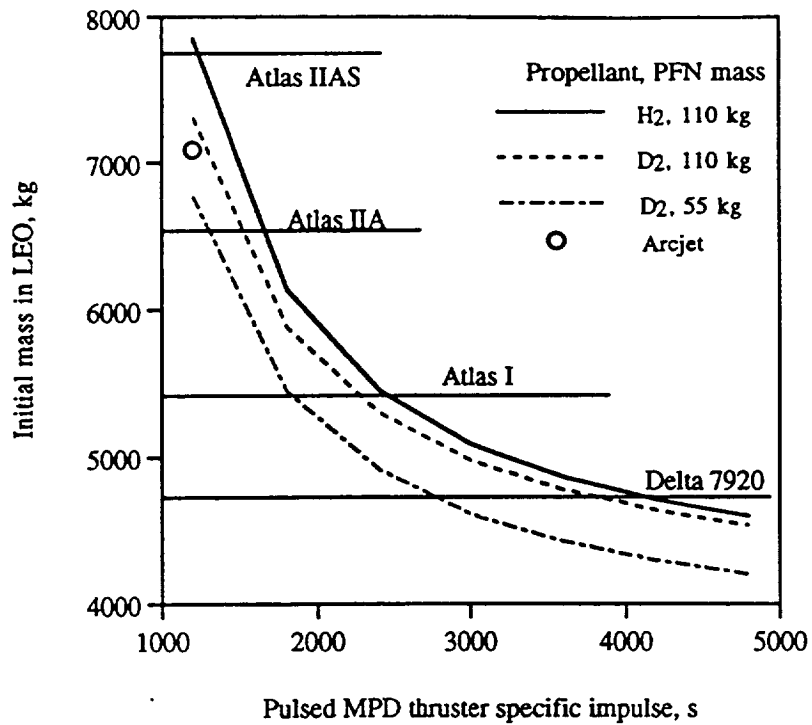


Fig. 12 - Effect of propellant choice and reduced PFN mass for a 40 kW spacecraft. 1000 kg payload, LEO - GEO transfer mission.

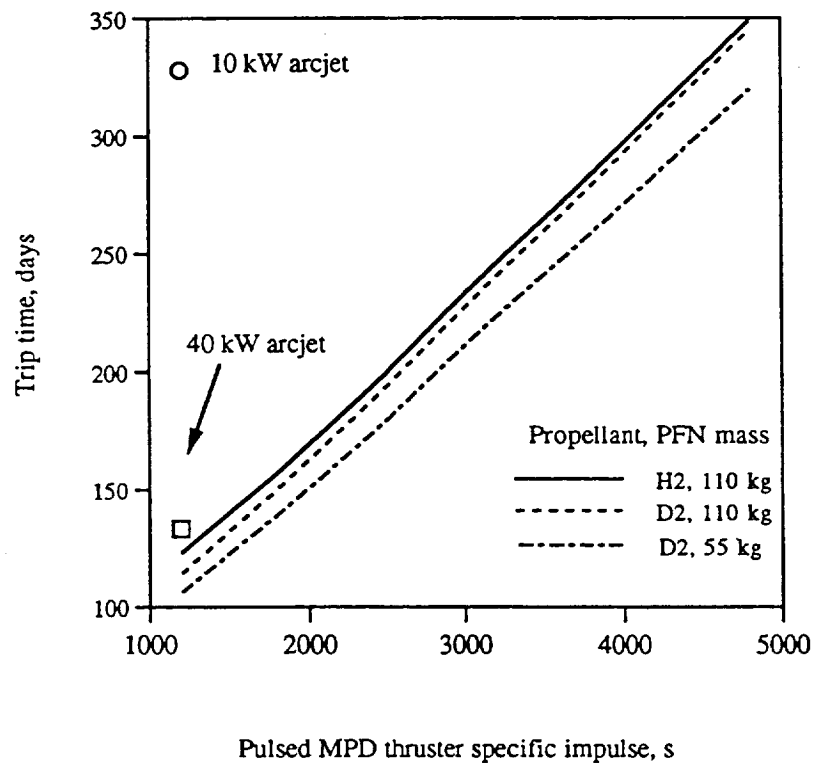


Fig. 13 - Impact of propellant choice and PFN mass on trip time as compared to H₂ arcjets. 1000 kg payload, LEO - GEO transfer mission.

REPORT DOCUMENTATION PAGE			Form Approved OMB No. 0704-0188	
Public reporting burden for this collection of information is estimated to average 1 hour per response, including the time for reviewing instructions, searching existing data sources, gathering and maintaining the data needed, and completing and reviewing the collection of information. Send comments regarding this burden estimate or any other aspect of this collection of information, including suggestions for reducing this burden, to Washington Headquarters Services, Directorate for Information Operations and Reports, 1215 Jefferson Davis Highway, Suite 1204, Arlington, VA 22202-4302, and to the Office of Management and Budget, Paperwork Reduction Project (0704-0188), Washington, DC 20503.				
1. AGENCY USE ONLY (Leave blank)		2. REPORT DATE September 1993		3. REPORT TYPE AND DATES COVERED Final Contractor Report
4. TITLE AND SUBTITLE Low Power Pulsed MPD Thruster System Analysis and Applications			5. FUNDING NUMBERS WU-506-42-31 C-NAS3-25266	
6. AUTHOR(S) Roger M. Myers, Matthew Domonkos, and James H. Gilland				
7. PERFORMING ORGANIZATION NAME(S) AND ADDRESS(ES) Sveredrup Technology, Inc. Lewis Research Center Group 2001 Aerospace Parkway Brook park, Ohio 44142			8. PERFORMING ORGANIZATION REPORT NUMBER E-8099	
9. SPONSORING/MONITORING AGENCY NAME(S) AND ADDRESS(ES) National Aeronautics and Space Administration Lewis Research Center Cleveland, Ohio 44135-3191			10. SPONSORING/MONITORING AGENCY REPORT NUMBER NASA CR-191187 AIAA-93-2391	
11. SUPPLEMENTARY NOTES Prepared for the 1993 Joint Propulsion Conference cosponsored by the AIAA, SAE, ASME, and ASEE, Monterey, California, June 28-July 1, 1993. Project Manager, James S. Sovey, Space Propulsion Technology Division, (216) 433-7454.				
12a. DISTRIBUTION/AVAILABILITY STATEMENT Unclassified - Unlimited Subject Categories 16, 20, and 75			12b. DISTRIBUTION CODE	
13. ABSTRACT (Maximum 200 words) Pulsed MPD thruster systems were analyzed for application to solar-electric orbit transfer vehicles at power levels ranging from 10 to 40 kW. Potential system level benefits of pulsed propulsion technology include ease of power scaling without thruster performance changes, improved transportability from low power flight experiments to operational systems, and reduced ground qualification costs. Required pulsed propulsion system components include a pulsed applied-field MPD thruster, a pulse-forming network, a charge control unit, a cathode heater supply, and high speed valves. Mass estimates were obtained for each propulsion subsystem and spacecraft component using off-the-shelf technology whenever possible. Results indicate that for payloads of 1000 and 2000 kg pulsed MPD thrusters can reduce launch mass by between 1000 and 2500 kg over those achievable with hydrogen arcjets, which can be used to reduce launch vehicle class and the associated launch cost. While the achievable mass savings depends on the trip time allowed for the mission, cases are shown in which the launch vehicle required for a mission is decreased from an Atlas IIAS to an Atlas I or Delta 7920.				
14. SUBJECT TERMS Magnetoplasmadynamic; Plasma dynamics; Electric propulsion			15. NUMBER OF PAGES 28	
			16. PRICE CODE A03	
17. SECURITY CLASSIFICATION OF REPORT Unclassified	18. SECURITY CLASSIFICATION OF THIS PAGE Unclassified	19. SECURITY CLASSIFICATION OF ABSTRACT Unclassified	20. LIMITATION OF ABSTRACT	